Nuclear Engineering and Technology 55 (2023) 1071–1083

Contents lists available at ScienceDirect

Nuclear Engineering and Technology

journal homepage: www.elsevier.com/locate/net

Original Article

On-the-fly energy release per fission model in STREAM with explicit neutron and photon heating

Nhan Nguyen Trong Mai, Woonghee Lee, Kyeongwon Kim, Bamidele Ebiwonjumi [1], Wonkyeong Kim, Deokjung Lee*

Department of Nuclear Engineering, Ulsan National Institute of Science and Technology, 50 UNIST-gil, Ulsan, 44919, Republic of Korea

ARTICLE INFO

Article history:
Received 30 August 2022
Received in revised form
30 October 2022
Accepted 6 November 2022
Available online 12 November 2022

Keywords:
Energy release model
Photon transport
STREAM

ABSTRACT

The on-the-fly energy release per fission (OTFK) model is implemented in STREAM to continuously update the Kappa values during the depletion calculation. The explicit neutron and photon energy distribution, which has not been considered in previous STREAM versions, is incorporated into the existing on-the-fly model. The impacts of the modified OTFK model with explicit neutron and photon heating in STREAM on the power distribution, fuel temperature, and other core parameters during depletion with feedback calculations are studied using several problems from the VERA benchmark suit. Overall, the explicit heating calculation provides a better power map for the feedback calculations particularly when strong gamma emitters are present. Generally, the fuel temperature decreases when neutron and photon heating is employed because fission neutrons and gamma rays are transported away from their points of generation. This energy release model in STREAM indicates that gamma energy accounts for approximately 9.5%–10% of the total energy released, and approximately 2.4%–2.6% of the total energy released will be deposited in the coolant for the VERA 5, NuScale, and Yonggwang Unit 3 2D cores.

1. Introduction

Approximations for the energy released in nuclear reactions have long been used to reduce the complexity and computational burden in the reactor core analysis [1-3]. The energy released of fissionable nuclides, i.e., Kappa values, are employed for the power calculation where fission energies are assumed to be deposited locally or smeared into the problem [1,4]. The additional energy released, such as from neutron capture reactions of fission products and actinides, and especially from neutron capture reactions of strong absorbers (Boron or Gadolinium) is often neglected or treated as a simple-averaged constant deduced from reactor operation data and independent of material compositions. However, it has been observed that such approximations can introduce errors and compromise the calculation accuracy [5]. The inaccuracy in the power calculations caused by the inadequate energy released from fission and neutron capture reactions has been addressed in CASMO5 [6] by introducing an energy release per fission model [5]. Fixed values for the energy released per neutron capture reaction of certain nuclides (i.e., from capture in hydrogen, boron, gadolinium, actinides, and fission products) are used instead of an averaged constant for all nuclides. In addition, the energy of fission fragments and betas, and the kinetic energy of fission neutrons are directly taken from the evaluated nuclear data file [7] in this model.

STREAM, developed by the Computational Reactor Physics and Experiment Laboratory (CORE) at the Ulsan National Institute of Science and Technology (UNIST), is a deterministic neutron-transport code specialized for the analysis of two-dimensional (2D) and three-dimensional (3D) reactor cores [8,9]. The default energy release model in STREAM simply uses constant Kappa values to account for the energy released from fission and capture reactions of fissionable nuclides while the energy released from neutron capture of non-fissionable nuclides is neglected. To improve the accuracy of STREAM, an on-the-fly energy release per fission (OTFK) model was implemented based on the concept

* Corresponding author.
E-mail addresses: mainhan@unist.ac.kr (N.N.T. Mai), dldndgml0310@unist.ac.kr (W. Lee), kyeongwon@unist.ac.kr (K. Kim), bamidele@mit.edu (B. Ebiwonjumi), poryor@unist.ac.kr (W. Kim), deokjung@unist.ac.kr (D. Lee).
[1] Bamidele Ebiwonjumi was affiliated with Department of Nuclear Engineering, Ulsan National Institute of Science and Technology, 50 UNIST-gil, Ulsan 44,919, Republic of Korea. He is now affiliated with Plasma Science and Fusion Center, Massachusetts Institute of Technology, Cambridge, MA 02139, USA.

https://doi.org/10.1016/j.net.2022.11.003

deployed in CASMO5. The microscopic cross-section data (capture, fission, Kappa) for all nuclides in all regions are stored and then used for the energy release calculation in CASMO5, which does not introduce memory issues in single-assembly problems. However, STREAM computes the Kappa value for each region in an equivalent formulation without the need to save the microscopic cross-section data of all regions, thus minimizing the memory required for a whole-core calculation [9]. STREAM inherits the local deposition assumption of gamma and neutron energies in this model.

The large gradient of neutron/photon flux distribution in core geometries featuring strong absorbers/emitters or leakage can deteriorate the accuracy of these assumptions. This is because neutron/photons are unlikely to be uniformly distributed in such problems and will most likely deposit their energies far away from their points of generation. Furthermore, the fraction of energy deposited in the coolant needed for thermal hydraulics (TH) feedback is missed because the locally deposited assumption places all the energy in the fuel regions. This fraction is often determined by user preferences. Accurate calculation of energy deposition and TH feedback requires explicit neutron/photon transport [10-12].

The gamma calculation has been considered in some deterministic codes such as MPACT [13], WIMS [14], nTRACER [15], and other Monte Carlo codes such as SERPENT [16] and OpenMC [17]; however, the literature is limited to small problems without depletion calculation or validation against measurement data. The coupled neutron/photon mode is also available in MCNP [18], McCard [19], and MCS [20], but the contributions of prompt gamma rays or delay particle energies are not explicitly computed in the calculations of criticality problems [21]. Recently, a photon module that used an explicit distribution calculation for the photon energy was implemented in STREAM to improve the power distribution accuracy [22]. The continuous update of the Kappa value during depletion with an explicit neutron/photon energy distribution is a more realistic model in reactor analysis for STREAM.

The principle of the OTFK model in STREAM is first presented, followed by an introduction of the explicit neutron/photon energy deposition calculation. The energy release models in STREAM are then verified against the results of other studies on lattice problems from the VERA benchmarks [23]. STREAM can compute the decay heat of irradiated fuel using an in-built source term module [24,25], which relies on the energy release model during the depletion calculation. Thus, the energy models in STREAM are validated by computing the decay heat of some assemblies from typical pressurized light water reactors (PWRs) and comparing them with measurement data. Subsequently, a comparison of the calculated parameters of several 2D cores, namely VERA [23], NuScale [26], and Yonggwang Unit 3 [27], is presented to quantify the impact of the energy model with explicit neutron and photon heating in STREAM.

2. On-the-fly energy release per fission model in STREAM and the modifications for the explicit neutron and photon heating

2.1. On-the-fly energy release per fission model

The concept of the OTFK model in STREAM has been mentioned in Ref. [9] and is explained as follows. The kappa value in STREAM for isotope i (MeV) is computed using the following equation:

$$\kappa_i^n \approx ER_i(0) - \delta ER_i(E^n) + \frac{R_c}{R_f}\overline{Q}_c = \kappa_i'^n + \frac{R_c}{R_f}\overline{Q}_c \tag{1}$$

where $ER_i(0)$ (MeV) is the total energy released per fission less the neutrino energy from the evaluated nuclear data file (MT458 in ENDF [7]). The kinetic energy of the fission fragments (*EFR*), delayed beta (*EB*), kinetic energy of prompt (*ENP*) and delayed (*END*) fission neutrons, energy of prompt (*EGP*) and delayed (*EGD*) fission gamma is stored in $ER_i(0)$. However, constituent terms of $ER_i(0)$ are incident-energy dependent. This dependence is approximated by an energy dependent function deduced from the Sher-Beck systematics [28] provided in reference [29]. Because the function for *EFR*, *EGP* and *END* are zero, the total function for $ER_i(0)$ is:

$$\delta ER_i(E^n) = \delta EB(E^n) + \delta EGD(E^n) + \delta ENP(E^n) = -1.157E^n + 8.07\left[\nu_i^n - \nu_i(0)\right] \tag{2}$$

where E^n is the average energy of incident neutron in group n and ν is the number of fission neutrons generated by incident neutron in the energy group n. The number of fission neutrons generated by incident neutron in the lowest-energy group is denoted as $\nu(0)$. The last term $\frac{R_c}{R_f}\overline{Q}_c$ is the average energy released from neutron capture reactions per fission, where $\frac{R_c}{R_f}$ represent the capture to fission ratio. The value of $\overline{Q}_c$ (MeV) is computed using Equation (3).

$$\overline{Q}_c = \frac{\sum_m \sum_i \sum_n q_{c,i} N_{m,i} \sigma_{c,m,i}^n \phi_m^n V_m}{\sum_m \sum_i \sum_n N_{m,i} \sigma_{c,m,i}^n \phi_m^n V_m} = \frac{\sum_m \sum_n q \Sigma_{c,m}^n \phi_m^n V_m}{\sum_m \sum_n \Sigma_{c,m}^n \phi_m^n V_m} \tag{3}$$

Where m is the region's index, and $q_{c,i}$ is the energy of the capture gammas and captured products of nuclide i. $N_{m,i}$ is the number density of nuclide i in region m, $\sigma_{c,m,i}^n$ is the capture cross-section, ϕ_m^n is the neutron flux, and V_m is the volume of region m. It is noted that the capture rate R_c in this work is computed with the neutron flux of the next generation $k\phi_m^n$ because the neutron capture energy (non-fission) is produced after fission events by interactions of newly born neutrons. The adjustment by the multiplication factor k is not applied to those stored in $ER_i(0)$ because these energies are directly released in each fission. The macroscopic cross-section for the term $\kappa_i'^n$ in Equation (1) is defined as:

$$\kappa' \Sigma_{f,m}^n = \sum_i N_{m,i} \kappa_i'^m \sigma_{f,m,i}^n \tag{4}$$

where $\sigma_{f,m,i}^n$ is the microscopic fission cross-section. The macroscopic cross sections $\Sigma_{c,m}^n$, $q\Sigma_{c,m}^n$, $\Sigma_{f,m}^n$, and $\kappa'\Sigma_{f,m}^n$ are computed and saved for use in the OTFK model. The energy released in region m is calculated as follows:

$$P_m = \sum_n \kappa \Sigma_{f,m}^n \phi_m^n V_m = \sum_n \left[\kappa' \Sigma_{f,m}^n + \frac{R_c}{R_f}\overline{Q}_c \Sigma_{f,m}^n\right] \phi_m^n V_m \tag{5}$$

In this OTFK model, the energy from fission fragments, fission gamma, fission neutron, betas are deposited locally whereas the energy from neutron capture reactions (kinetic energy of captured products and gamma energy) is distributed to all fuel regions and proportional to the capture rate in those regions by the term $\frac{R_c}{R_f}\overline{Q}_c$ in Kappa values. Because the energy deposition is only computed for fuel regions, the fraction of energy deposition in the coolant for thermal hydraulics calculation (obtained by dividing the amount of energy deposited in the coolant by the total energy released in the problem) is defined by user experience.

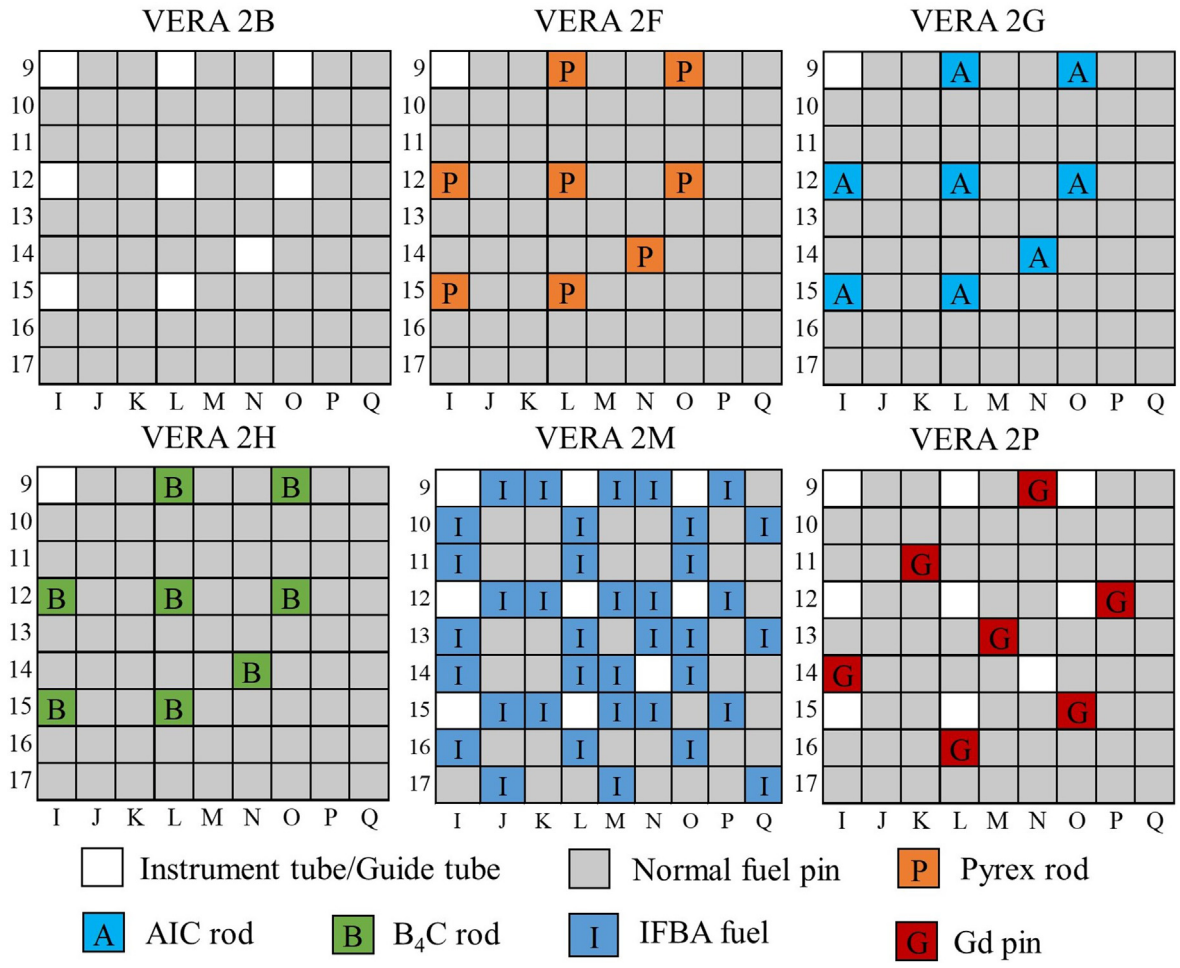

Figure 1. Layout of the VERA lattice problems.

Table 1
Average energy released per fission for VERA 2B computed by MCS in comparison to MCNP and SERPENT in Ref. [16].

Component	MCS (MeV)	MCS − MCNP (keV)	MCS − SERPENT (keV)
Fission products + neutrons	173.428	−72.2	+61.8
Beta	6.611	−31.0	+1.0
Prompt fission gamma	6.568	−8.4	−0.4
Delayed fission gamma	6.399	−23.5	+27.5
Capture gamma	6.311	+11.7	+1.7
Total	199.317	−123.3	+91.7

2.2. Modifications of the OTFK model with explicit neutron and photon heating

When photon transport is enabled in STREAM, the Kappa value is modified by changing the $ER_i(0)$ values in Equation (1) and $q_{c,i}$ values in Equation (3). The contribution of prompt and delayed fission gamma rays $(EGP+EGD)$ in the $ER_i(0)$ is removed, and the prompt photon energy from neutron capture in $q_{c,i}$ is set to zero. The gamma source is then computed, and photon transport is performed to calculate the photon heating in each region. The implementation of the photon transport module and photon library in STREAM are presented in Refs. [22,30].

The energy deposition from the neutron slowing down and energy of neutron-captured products are also considered explicitly in this modified OTFK model. The kinetic energy of the fission neutrons $(ENP+END)$ stored in $ER_i(0)$ is removed and the energy of

Table 2
Multiplication factors from STREAM in comparison to those from MCS*

Problem	Burnup	STREAM	STREAM − MCS (pcm)
VERA 2B	BOC	1.18204	−93
	MOC	0.90087	+86
	EOC	0.77438	+110
VERA 2P	BOC	0.92707	+31
	MOC	0.87953	+70
	EOC	0.74406	+68

*Standard deviation from MCS is less than 7 pcm.

Table 3
Average energy released (MeV/fission) from STREAM compared to MCS (STREAM − MCS in keV/fission is given in the brackets).

VERA	Burnup	MCS	CONSTK	OTFKCQ	OTFKVQ
2B	BOC	199.317	202.991 (+3674.5)	199.505 (+188.6)	199.291 (−25.9)
	MOC	206.480	208.644 (+2163.2)	206.895 (+414.8)	206.405 (−75.2)
	EOC	209.462	210.966 (+1053.4)	209.939 (+477.1)	209.388 (−74.7)
2P	BOC	201.912	203.116 (+1203.7)	202.141 (+229.2)	201.888 (−24.4)
	MOC	206.520	208.660 (+2140.1)	206.865 (+345.4)	206.421 (−98.8)
	EOC	209.588	211.067 (+1479.1)	210.005 (+416.2)	209.490 (−98.7)

Table 4
The error (OTFKCQ − MCS) in keV for VERA 2B.

Component	BOC	MOC	EOC
Neutron	+306.7	+418.8	+408.4
Gamma	−116.9	+25.7	+145.7
Neutron + Gamma	+189.7	+444.5	+554.1

captured products in $q_{c,i}$ are also removed. With explicit photon/neutron calculation, only energies of some daughter nuclides from decay process of capture products remain in $q_{c,i}$. In addition, the correction terms in Equation (1) are adjusted to account for the removal of photon and neutron energies from $ER_i(0)$. Because only EFR and EB remain in $ER_i(0)$ and $\delta EFR = 0$, Equation (2) can be modified as:

$$\delta ER_i(E^n) = \delta EB = 0.075E^n \tag{6}$$

The energy deposition in each region is computed with Equation (7)

$$P_m = \sum_n \left[\kappa^{*'} \Sigma^n_{f,m} + \frac{R_c}{R_f} \overline{Q}^*_c \Sigma^n_{f,m} \right] \phi^n_m V_m + \sum_n k \Sigma^n_{heat} \phi^n_m V_m + \sum_p \Sigma^p_{heat} \phi^p_m V_m \tag{7}$$

where ϕ is the flux of neutrons (n) or photons (p), and Σ^n_{heat} and Σ^p_{heat} is the neutron and photon heating cross-section, respectively (computed by NJOY [31]). The superscript * denotes the modified values after the removal of photon and neutron energies, as previously mentioned.

Because the kinetic energy of fission fragments is already in $ER^*_i(0)$ term, the neutron heating cross-section is equal to the total heating cross-section (MT301) minus the fission heating cross-section (MT318) [16]. It is noted that the gammas source from neutron capture reactions is adjusted by the multiplication factor k before the photon transport calculation. The role of k for the capture gamma energy has been explained previously. The kinetic energy of fission neutrons is no longer saved in $ER_i(0)$ but computed separately based on the neutron flux. Thus, the neutron heating quantities (non-fission) is also multiplied by k because of the same reason applied to capture gamma energies. The fraction of energy deposition in the coolant is no longer required because the energy deposition in each material, such as the fuel, cladding, and coolant, is available with this approach.

3. Results and discussions

3.1. VERA lattice problems

VERA 2B, 2F, 2G, 2H, 2M, and 2P, which represent typical problems in calculation with PWRs, were selected from the VERA benchmark suite [23]. The VERA lattice problems are 17 × 17 assemblies. The configuration of these problems is shown in Fig. 1, and all calculations were conducted with ENDF/B-VII.1 library [7].

3.1.1. Verification with MCS

The Monte Carlo code MCS [20,32] developed at UNIST was used to verify the energy models in STREAM. The neutron and photon heating were tallied during the criticality runs in the coupled neutron/photon mode of MCS, but additional post-processing steps were required to obtain the proper neutron/photon energy components. Details of the post-processing steps known as the k correction method were well explained in the references [16,33]. At first, the energy released for VERA 2B problem computed by MCS are compared to those from MCNP and SERPENT reported in the reference [16] to verify the MCS calculations. The comparison for MCS results is given in Table 1. Statistical error of MCS is below 0.05% and is thus not shown. MCS results are in good agreement with reference values.

The energies deposition in VERA 2B and 2P were then computed to verify the energy model in STREAM. The error (defined as STREAM − MCS in keV) of these two problems was investigated at three burnup steps, namely 0 MWd/kg (beginning of cycle BOC), 30 MWd/kg (middle of cycle MOC), and 60 MWd/kg (end of cycle EOC). The depleted number densities were first generated by the depletion module in MCS and used in STREAM calculations to ensure the consistency in the input material compositions. It is noted that the contribution of energies from decay nuclides in $q_{c,i}$ is set to zero for comparison purposes since the decay calculation are not available for Monte Carlo codes such as MCS or MCNP. In addition, each VERA problem was run three times in STREAM. The first run employed the default model, and the second run employed the conventional OTFK model where no explicit neutron and photon heating was involved, and the third run included the modified OTFK model with explicit neutron and photon heating.

The default model in STREAM uses constant Kappa and is abbreviated as CONSTK. The conventional OTFK model places all energy components in Kappa where constant q values are used for the energy released from neutron capture (as in Equation (1)). Thus, this model's name is abbreviated as OTFKCQ. In contrast, the energy released by neutron capture is not constant but varied with the explicit neutron and photon calculation in the modified OTFK model. Therefore, the new model is abbreviated as OTFKVQ. For the rest of the paper, these abbreviations are utilized to indicate the three available models in STREAM. Furthermore, STREAM is assumed to be in the CONSTK, OTFKCQ, and OTFKVQ modes when the CONSTK, OTFKCQ, and OTFKVQ energy models are respectively employed. Values of the multiplication factors of VERA 2B and 2P are given in Table 2. The average energy released computed by different models in STREAM for these two problems are compared with MCS in Table 3.

The CONSTK model over predicted the energy released in all cases because reference values from MCS are computed with an explicit neutron-photon heating scheme instead of using generic constant Kappa values as in the CONSTK model. Excellent agreement between CONSTK model and MCS was observed if same

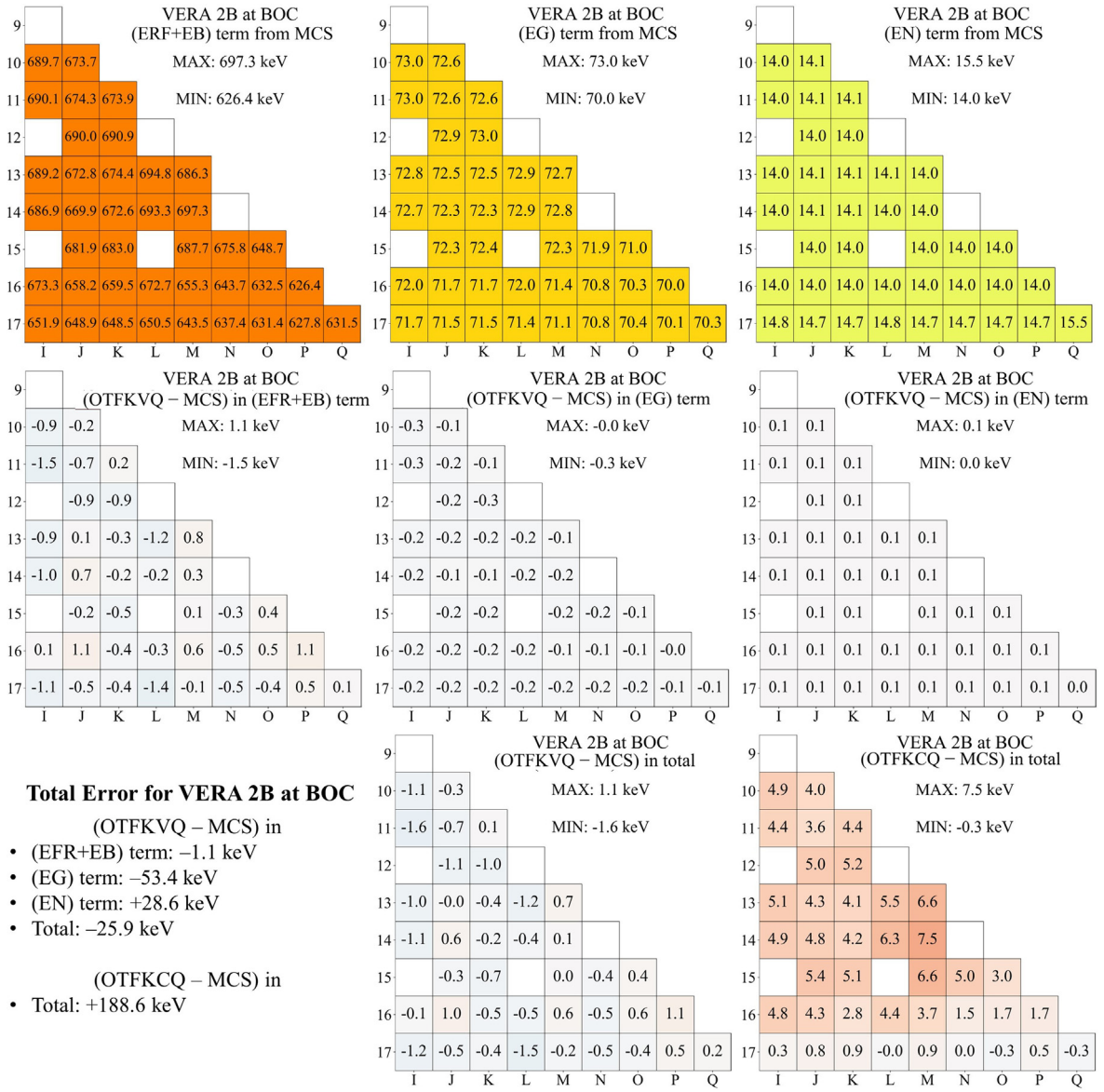

Figure 2. Comparison between the OTFKVQ and OTFKCQ model to MCS for VERA 2B at BOC.

generic Kappa values were used in both codes. The energy released from OTFKVQ mode was slightly lower compared to MCS at later burnup steps. The OTFKCQ mode induced a difference of few hundreds keV per fission compared to MCS.

The discrepancies observed between MCS and OTFKCQ model was a net result of several tangled factors. Firstly, the neutron energy in the OTFKCQ model is computed based on a constant neutron energy released for each nuclide, a. k.a (*ENP*+ *END*), adjusted with correction terms to account for different incident neutron energy as in Equation (1). Secondly, the neutron capture energy in the OTFKCQ model was assumed to be independent of incident neutron energies and equal to the energy released from thermal neutron capture. Thirdly, it was pointed out in the reference [16] that the prompt fission gamma spectrum and the prompt fission gamma multiplicity for ^{235}U and ^{238}U in the ENDF/B-VII.1 library [7] is not consistent with the fission gamma energy in MT458 data. The fission gamma of ^{235}U above 1.09 MeV incident neutron energy is also lumped with the gamma from other reactions in ENDF/B-VII.1 [16]. Thus, the OTFKCQ model computes the gamma energy based on MT458 data and correctly preserves the total fission gamma energy whereas inconsistency will arise in the OTFKVQ mode and MCS, especially when the *k* value deviates from unity. In contrast, the neutron energy in the OTFKVQ mode and MCS is computed without approximations. Thus, the separation of each component in neutron or gamma energy in the OTFKCQ and MCS for an exact comparison is virtually unfeasible. The lumped error for neutron and gamma energy calculated by the OTFKCQ model compared to MCS are provided in Table 4 for VERA 2B.

Inconsistency in the gamma energy will be alleviated with the ENDF/B-VIII.0 library because the prompt fission gamma spectrum and the prompt fission gamma multiplicity for ^{235}U and ^{238}U has been corrected to be consistent with MT458 data [16,34]. Still, the error occurred in the kinetic energy of fission neutrons would remain. The pin power distribution computed with OTFKCQ and OTFKVQ mode is now compared to those obtained from MCS. The OTFKVQ model was verified in three separate components indicated in Equation (7), namely:

- the energy from fission fragments and delayed betas (denoted as $EFR + EB$).

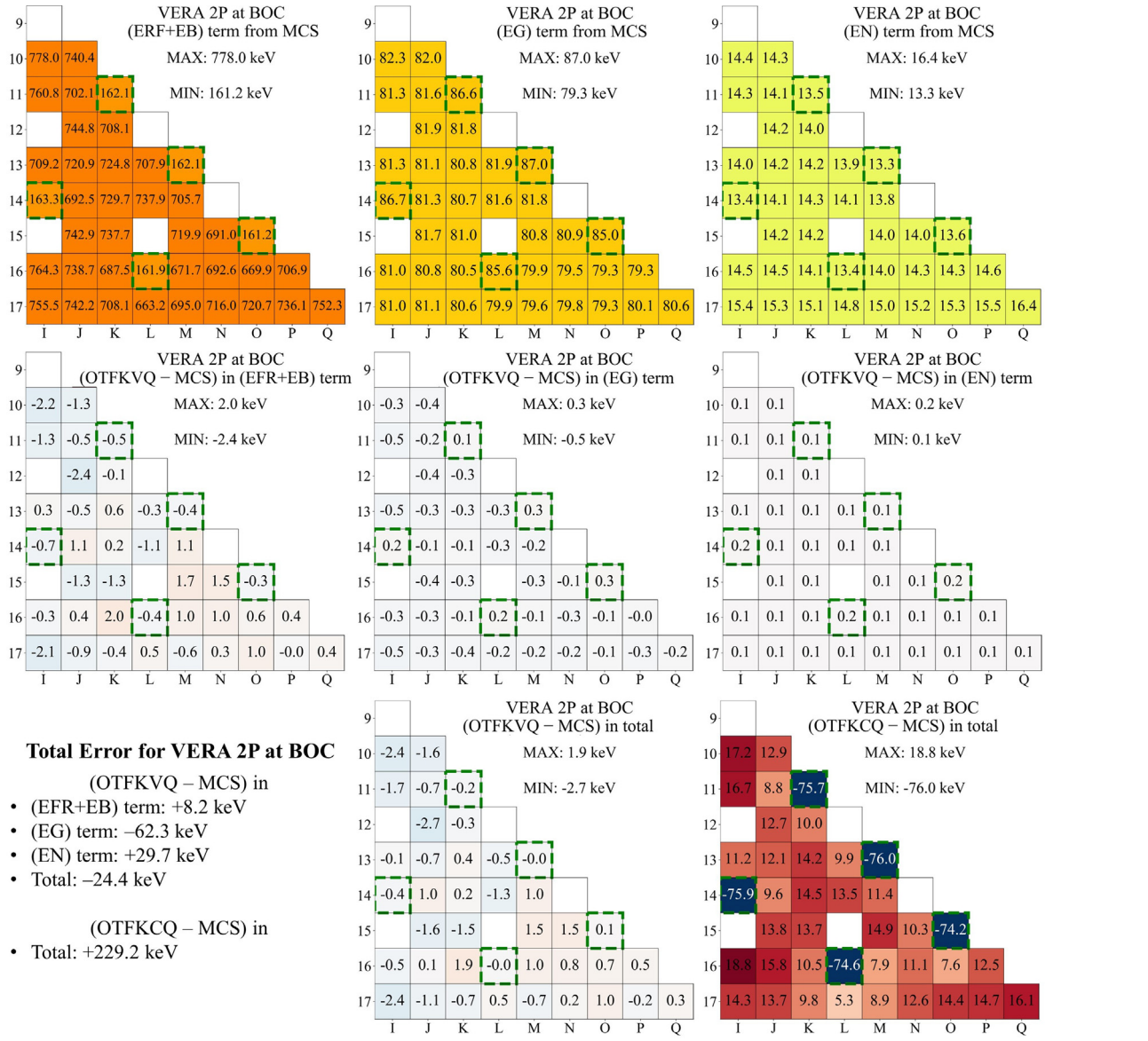

Figure 3. Comparison between the OTFKVQ and OTFKCQ model to MCS for VERA 2P at BOC (Gadolinia pins are marked by dashed-green boxes).

- the energy from neutrons (denoted as *EN*).
- the energy from gammas (denoted as *EG*).

The OTFKCQ model lumps the energy of fission fragments, beta, fission neutron and fission gamma in $ER_i(0)$. Thus, the comparison for the OTFKCQ model is only for the total pin power. Comparison for VERA 2B and VERA 2P at BOC is presented in Figs. 2 and 3, respectively while those for MOC and EOC are given in the supplement data.

Good agreement was shown for the OTFKVQ mode with the error within ±2.6 keV compared to MCS. The OTFKCQ mode, however, introduced some discrepancies in both VERA problems. The contribution of gamma from Gadolinia pins was reduced by ~75 keV in the OTFKCQ mode. Gadolinium (Gd) emits a very strong gamma beam of 8 MeV per neutron capture reaction. In the OTFKCQ mode, these gamma energies would be divided into all fuel pins as explained in section 2.1. As a results, normal fuel pins received additional energies while Gd pins loss some of its gamma power. At later burnup, the OTFKVQ mode were in good agreement with MCS (within ±0.8 keV for the *EG* and *EN* term), and the OTFKCQ still slightly overestimated the total energy released.

The calculation of energy components with Monte Carlo code required tremendous number of histories to achieve a reasonable statistical error. Thus, the normalized pin-power distributions by the OTFKVQ mode for remaining VERA problems were compared to those already reported in the reference [13] by MCNP and MPACT code. The relative error with MCNP and MPACT is presented in Figs. 4 and 5, respectively.

A good agreement was found between OTFKVQ mode, MCNP, and MPACT, except for the VERA 2G problem with the AIC control rod. It was explained in Ref. [22] that significant discrepancies in the gamma source generated in the AIC material are due to the inadequate resonance treatment in STREAM for nuclides, such as ^{109}Ag in the AIC. The pin-based point-wise energy slowing-down method in STREAM for resonance treatment [35] is only applied to fuel regions, and the extension of this method to non-fuel regions instead of the equivalent theory would alleviate such issues in the future. However, the OTFKVQ mode in STREAM shows better accuracy than MPACT in

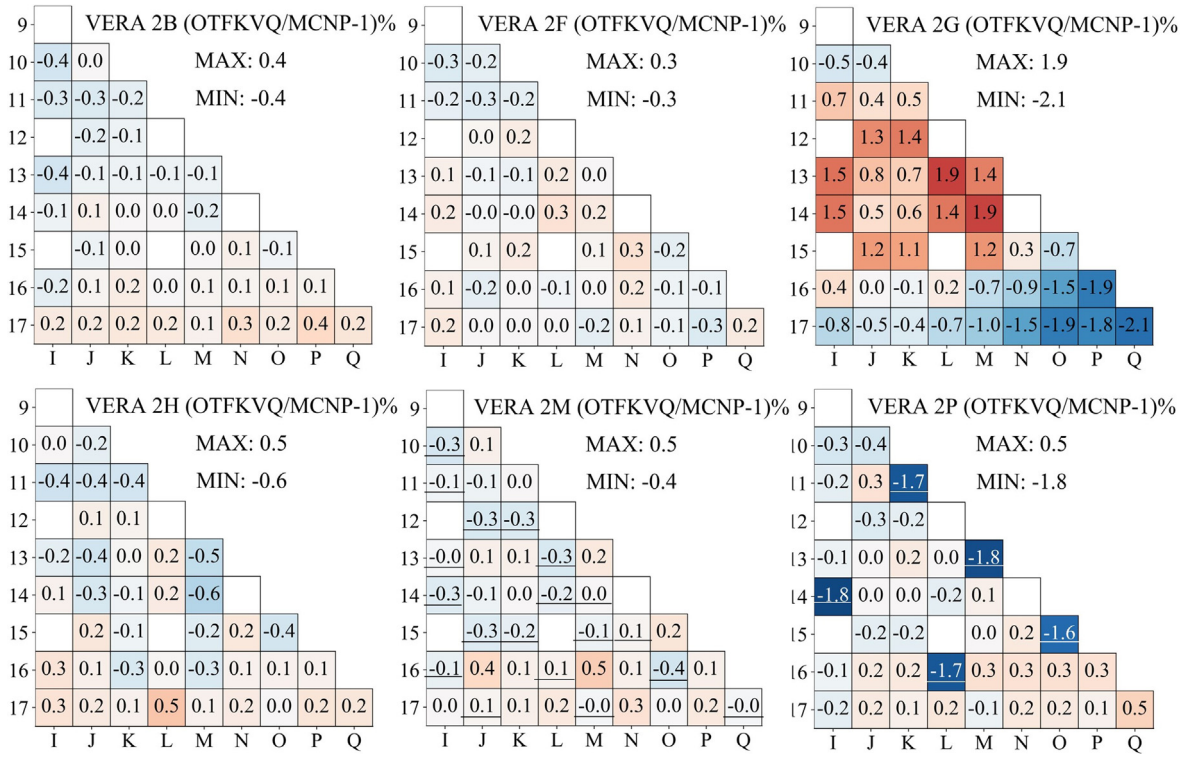

Figure 4. Comparison of the normalized pin-wise power obtained by OTFKVQ mode to those from MCNP (IFBA or Gd pins are underlined).

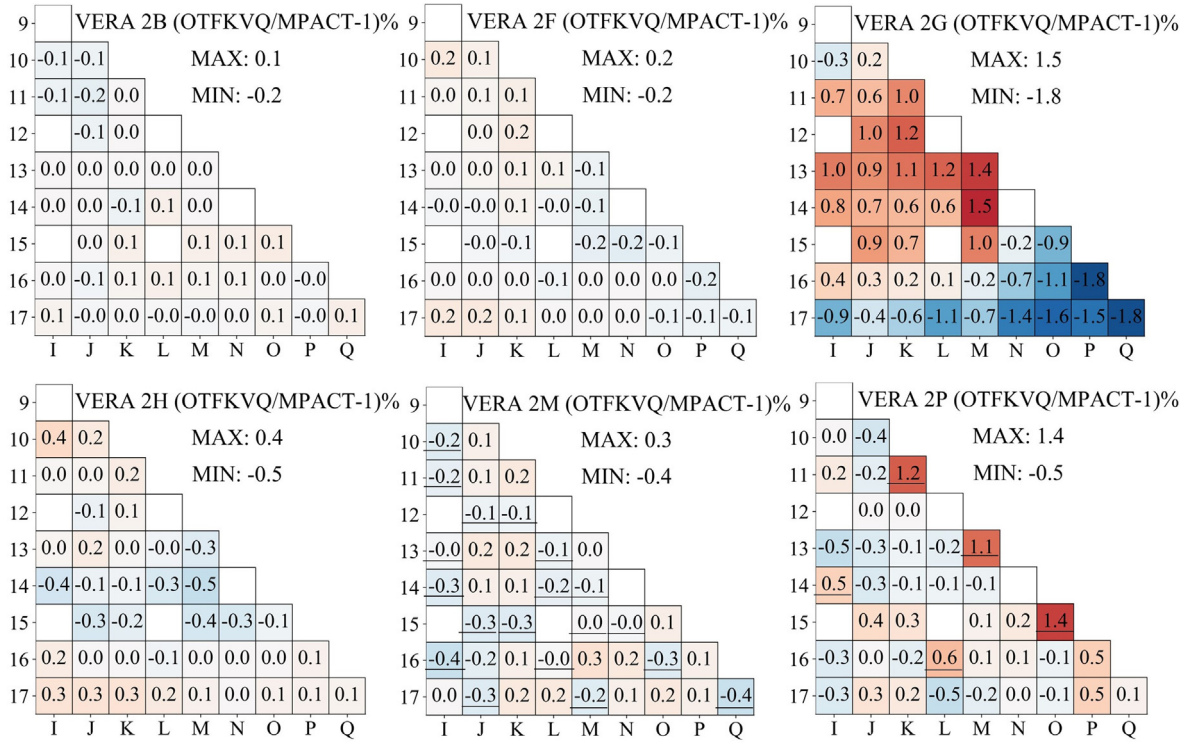

Figure 5. Comparison of the normalized pin-wise power obtained by OTFKVQ mode to those from MPACT (IFBA or Gd pins are underlined).

the case of VERA 2P. Because MPACT only applied a smearing scheme, distribution of high energy gamma emitted from Gd will not be accounted for adequately and an underestimation of −2% for Gad pin occurs when comparing MPACT to MCNP results. The fractions of energy deposition for VERA 2B in each material region obtained with the OTFKVQ mode were also in good agreement with values

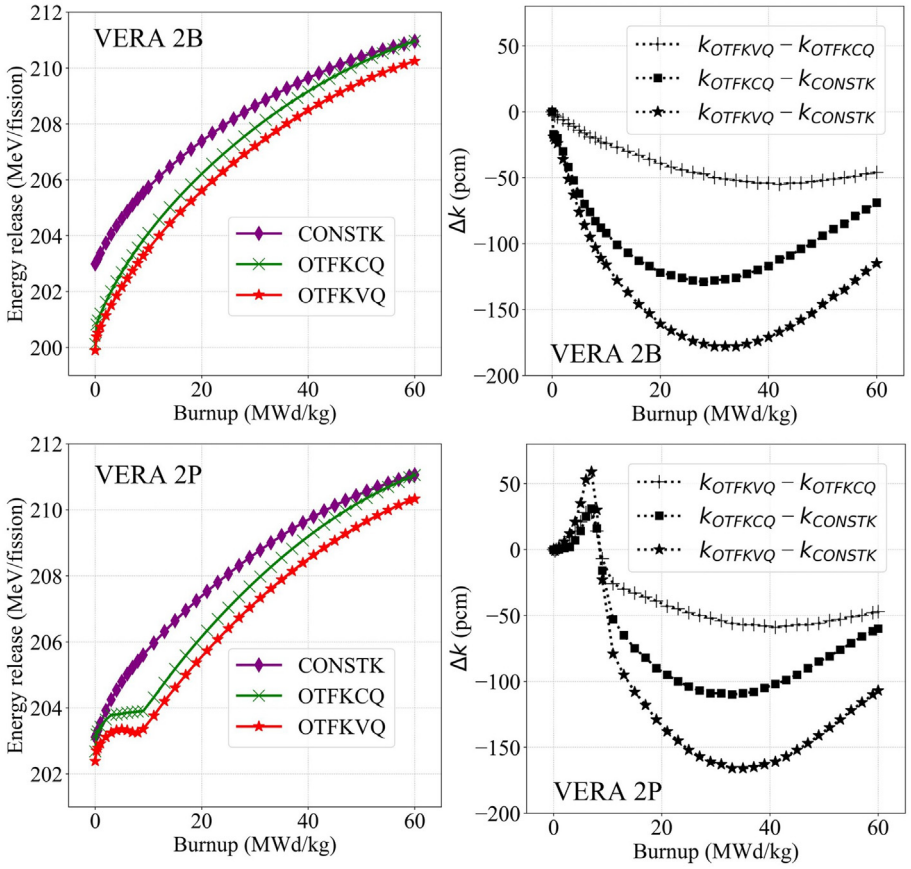

Figure 6. Energy release per fission and the difference in the multiplication factor for VERA 2B and VERA 2P for the three energy release models in STREAM.

calculated by OpenMC and reported in Ref. [36], where approximately 2.5% of the total energy is deposited in the coolant.

3.1.2. Impact of energy release model on burnup calculation

VERA 2B and VERA 2P were considered further during the burnup calculation in STREAM to analyze the impacts induced by different energy release models. It is noted that the contribution of delay energies in $q_{c,i}$ of the OTFKCQ and OTFKVQ mode was non-zero starting from this section and the depleted number densities were computed in STREAM corresponding to the predicted power level provided by each model. The impact of constant Kappa values and neglecting the gamma energy from neutron capture of Gd in the CONSTK mode compared to updated Kappa values can be observed during depletion by comparing the average energy released per fission and the change in the multiplication factor, as shown in Fig. 6.

As shown in Fig. 6, the multiplication factor for the CONSTK mode exhibits a maximum differences of 128 and 174 pcm between it and those obtained in the OTFKCQ and OTFKVQ modes, respectively. With the OTFKCQ and OTFKVQ mode, the average energy released in VERA 2P exhibits a plateau before 10 MWd/kg, corresponding to the burnout point of Gd [37]. Gamma rays generated from Gd contribute a significant fraction in the *EG* term (~8 MeV/capture). The depletion of Gadolinium reduces this contribution while the increasing gamma energies released from the buildup of fission products balance this loss. The CONSTK mode neglects the q values of non-fissionable nuclides and dose not capture this effect. After this burnup point, the difference between the CONSTK mode and the two other modes was comparable to that of the VERA 2B case. In general, a higher energy release is obtained in the CONSTK mode, which introduces an overestimation in the multiplication factor value (higher power released per fission indicates that less fuel will be burned to generate a certain power level, thus leading to a higher multiplication factor).

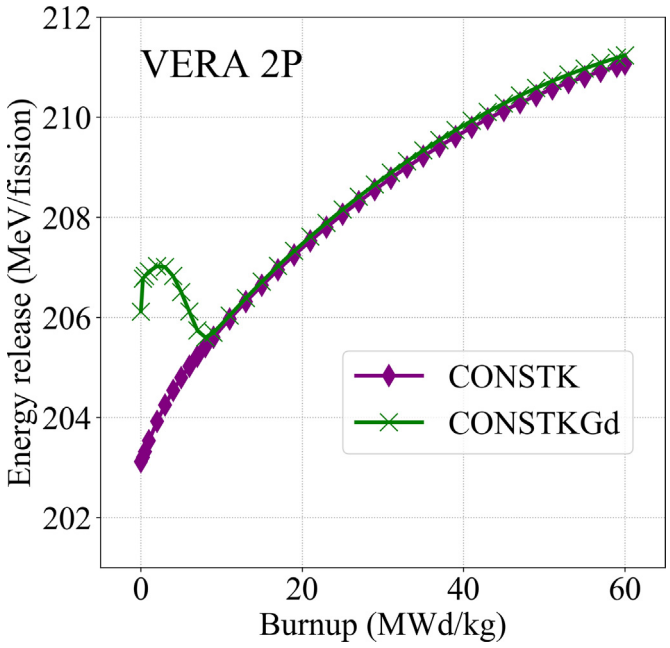

Figure 7. Energy release per fission when energy from neutron capture of Gd is added into CONSTK mode (abbreviated as CONSTKGd).

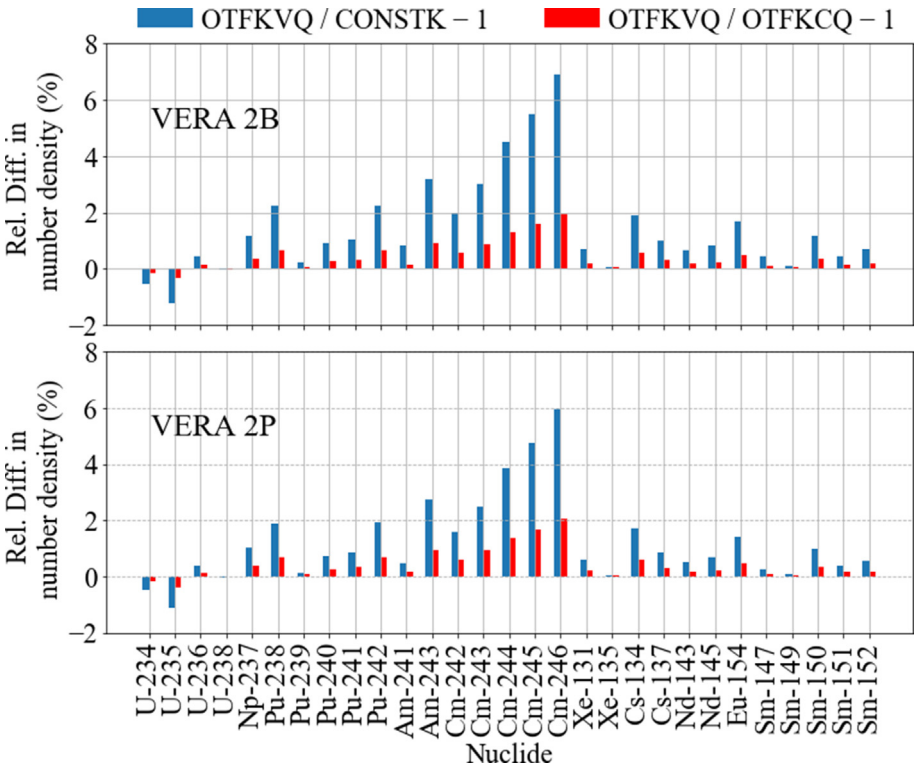

Figure 8. Relative difference (unit: %) in the total number density of some nuclide from the OTFKVQ mode compared to the OTFKCQ and CONSTK modes.

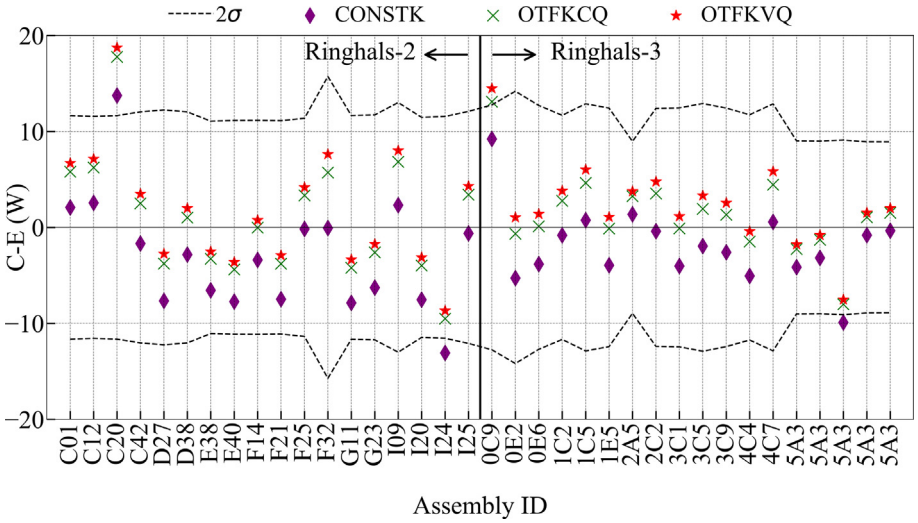

Figure 9. Differences in the decay heat calculated with different energy release models in STREAM compared to the measurement data (unit: watts).

Table 5
RMSE for the decay heat calculated by STREAM.

Reactor name	Energy release model in STREAM		
	CONSTK	OTFKCQ	OTFKVQ
Ringhals-2	6.6	6.2	6.5
Ringhals-3	4.3	4.3	4.8
Overall	5.5	5.3	5.7

The difference in k value between the OTFKCQ and the OTFKVQ mode is insignificant (maximum of ~50 pcm) because the energy released computed from these two models are quite closed to each other as shown previously in Table 3.

If the energy release from neutron capture of Gd is added in the CONSTK model, the effect of the Gd burnout can be observed in Fig. 7. The difference in the multiplication factor between the CONSTK mode and the CONSTK mode with added Gd can exceed 600 pcm before 10 MWd/kg. This difference is reduced to less than 50 pcm at later burnup steps. The CONSTK mode overestimates the energy release as indicated previously. Thus, the introduction of q values of other non-fissionable nuclides will further exacerbate this overestimation.

The difference in the multiplication factor is highest around the MOC. Thus, the relative differences in the total number density of

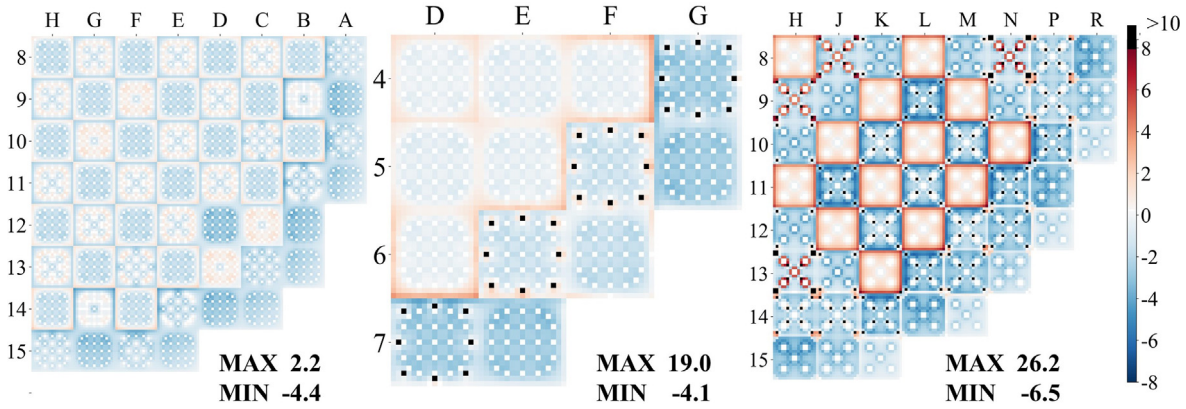

Figure 10. Difference (unit: watts) in pin power between the OTFKVQ and OTFKCQ modes at BOC (on the same color scale).

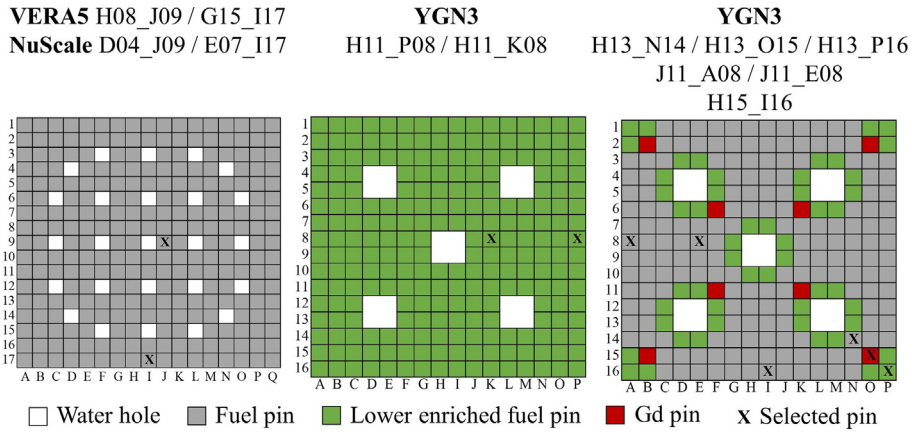

Figure 11. Locations of selected fuel pins.

Table 6
The power (in watts) of selected fuel pins computed in the OTFKVQ mode and the total difference compared to the OTFKCQ mode.

Pin ID	Material region			OTFKVQ − OTFKCQ
	Water	Cladding	Fuel	
H11_P08	4.2	1.7	138.3	+4.0
H11_K08	4.0	1.6	156.0	+0.7
J11_A08	4.4	1.9	229.7	−5.2
J11_E08	4.6	2.0	218.9	−2.6
H13_N14	4.8	2.1	227.9	−2.1
H13_O15	4.8	2.6	47.0	+24.4
H13_P16	4.7	2.1	135.4	+8.6
H08_J09	4.5	1.7	206.1	−2.0
D04_J09	4.9	1.9	208.6	−0.4
H15_I16	2.1	1.0	113.5	−2.0
G15_I17	2.0	0.8	99.3	−1.6
E07_I17	2.1	0.8	106.2	−2.0

some nuclides in the VERA 2B and 2P problems at this burnup step obtained in the OTFKVQ mode were compared to those obtained in the OTFKCQ and CONSTK modes. These differences are illustrated in Fig. 8.

The CONSTK mode resulted in a higher number of ^{235}U than the OTFKVQ mode for both VERA problems (+1.1% to +1.3%). The production of actinides and fission products is lower when the CONSTK mode is used, i.e., less fuel is burned. The fuel is slightly more depleted in the OTFKVQ mode than in the OTFKCQ mode because the average energy released per fission in the OTFKVQ mode is few hundreds keV lower than in the OTFKCQ. The highest difference between the results obtained with the OTFKVQ mode and other modes occurs for the *Cm* family, with a maximum of +7.2% for the CONSTK mode and +2.2% for the OTFKCQ mode. However, the number of *Cm* atoms is trivial compared to that of other actinides, as their density is approximately ten to one hundred times lower.

3.2. Decay heat calculation of PWR fuel assemblies

The decay heat module in STREAM has been verified and validated in several studies; however, only the CONSTK model has been considered [24,25,38]. The decay heat calculations of several assemblies from the Ringhals-2 reactor (15 × 15 assembly) and the Ringhals-3 reactor (17 × 17 assemblies) studied in previous works were tested again with the OTFKCQ and OTFKVQ model. The details of these assemblies are presented in Refs. [39,40]. The calculated decay heat values are provided separately in Table A1 in Appendix A, and the agreement between the calculated results and measurement data (within 2σ bounds) is shown in Fig. 9.

The root mean square error (RMSE) of the decay heat is computed as

$$RMSE = \sqrt{\frac{\sum_{i=1}^{n} (C_i - E_i)^2}{n}} \quad (8)$$

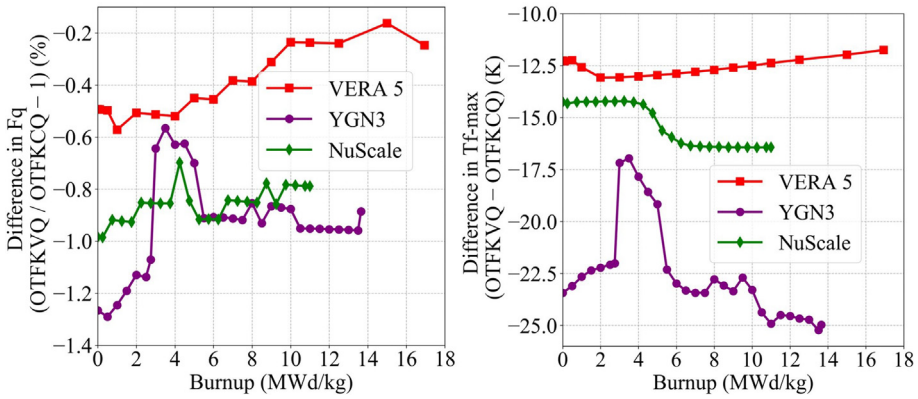

Figure 12. Differences in the peaking power factor (Fq) and fuel centerline temperature (Tf_max) obtained with the OTFKVQ and OTFKCQ models.

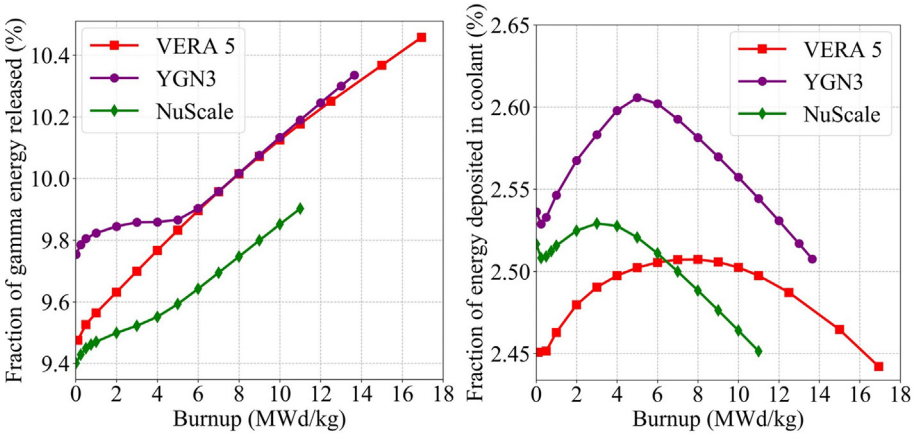

Figure 13. Fraction of gamma energy released, and the fraction of energy deposited in the coolant.

where C_i is the calculated decay heat from STREAM, E_i is the measured value of assembly i, and n is the number of assemblies. The RMSE values are presented in Table 5.

The OTFKCQ mode had the smallest RMSE value while the performance of the OTFKVQ mode was slightly lower. The energies released from decay processes of capture products were approximated in $q_{c,i}$ instead of being explicitly calculated. Although the energy released from the CONSTK and OTFKCQ model was overestimated compared to MCS, it could partially compensate the decay energies of capture products in $q_{c,i}$. Solution of Bateman equations would be necessary to quantify the impact of these decay sources. Overall, the decay heat calculated in all modes agreed well with the measurement data.

3.3. Analysis of 2D cores

Analysis was conducted for the 2D VERA5 [23], NuScale [26] and Yonggwang Unit 3 (YGN3) cores [27]. Compared to the VERA core, where Pyrex is used, the NuScale and YGN3 cores utilize Gd pins with Gd contents of 3 and 4 wt%, respectively. In addition, the NuScale core is a small modular reactor that utilizes a heavy stainless-steel reflector. The difference in pin power obtained in the OTFKCQ and OTFKVQ modes (defined as OTFKVQ − OTFKCQ) at the BOC for these cores is illustrated in Fig. 10. The CONSTK model was not considered in the analyses described in this section.

The significance of photon transport in the power map is case dependent. In general, the differences for normal fuel pins are small if they are not adjacent to strong gamma emitters such as Gd, higher enriched fuel pins, or if they are located at the core periphery where leakage is more profound than in the inner core regions. The power in fuel pins of selected assemblies depicted in Fig. 11 is presented in Table 6. The pin ID indicated in Table 6 and Fig. 11, for example, H11_P08 indicates fuel pin P08 in assembly H11.

The averaging of gamma energy from neutron captures to all fuel pins in the OTFKCQ model incurred a large reduction in the power of Gd pins as shown for the case of H13_O15. The fuel zoning can also affect the accuracy of the OTFKCQ mode when energies of fission neutron and fission gammas are assumed to be deposited locally. These neutrons/photons, in fact, can traverse to neighboring assemblies with lower photon/neutron source intensities. The difference for pin H11_P08 (low-enriched fuel) and J11_A08 (high-enriched fuel) located in two adjacent assemblies is an example for this effect. The comparison of the power peaking factor (Fq) and fuel centerline temperature (Tf-max) of the VERA, NuScale, and YGN3 2D cores is shown in Fig. 12.

In the OTFKVQ mode, the power peaking factor (Fq) is mostly lower than that obtained in the OTFKCQ mode and is more noticeable for the NuScale and YGN3 cores, where it is reduced by −0.9% and −1.3%, respectively. The reduction in Fq in the neutron/photon calculation might allow more loading patterns to be considered during the safety analysis. The change in centerline fuel temperature is insignificant for the VERA and NuScale cores, with a reduction of 12 K−16 K, whereas an average reduction of more than 20 K occurs for the Gd pins for YGN3. However, the temperature change is insignificant to induce the Doppler effect. Other parameters, such as the critical boron concentration (CBC)

and coolant temperature, are virtually unaffected when switching from the OTFKCQ mode to the OTFKVQ mode. The fractions of gamma energy released and deposited in the coolant are shown in Fig. 13.

The fraction of gamma energy released, and the fraction of energy deposited in the coolant of the NuScale core is slightly lower than those of the other two cores. In general, the fraction of gamma energy released is approximately 9.5%–10.5% of the total energy released, and the fraction of energy deposited in the coolant of PWRs can be set as 2.5%–2.6%, as deduced from Fig. 13.

4. Conclusion

The on-the-fly energy release per fission model (OTFK) was implemented in STREAM to consider the energy released from neutron capture reactions and the change in Kappa values during depletion. The upgraded OTFK model with explicit neutron and photon heating were studied on some VERA 2D benchmark problems and validated against decay heat measurements of assemblies in typical PWRs. The results obtained with the explicit neutron and photon heating in STREAM exhibited good agreement with the reference values.

The impact of this new model on the reactor analysis is more apparent when large gradient of neutron/photon flux distribution occurs. The power peaking factor exhibited a relative difference of −1.3% and −0.9% for the YGN3 and NuScale cores, respectively, at BOC, and these differences are reduced at later burnup when the explicit neutron and photon heating is incorporated. From the study of the 2D cores, gamma energy accounts for 9.5%–10% of the total energy released, and calculations with STREAM confirm the usage of the ~2.6% designated as the fraction of energy deposited in the coolant of typical PWRs. This new energy release model also introduces a better power map for TH calculation, especially when strong gamma emitters such as Gadolinium are present.

Future studies will focus on analyses of 3D problems, especially when gadolinia is introduced in the core, and comparisons to measurement data to further verify this energy release model in STREAM. In addition, the energy release models will be assessed for boiling water reactors (BWRs) once the capabilities for solving BWR problems are available in STREAM.

Declaration of competing interest

The authors declare that they have no known competing financial interests or personal relationships that could have appeared to influence the work reported in this paper.

Acknowledgments

This work was partially supported by the National Research Foundation of Korea (NRF) grant funded by the Korea government (MSIT) (No. NRF-2019M2D2A1A03058371). This work was also partially supported by the project (L20S089000) by Korea Hydro & Nuclear Power Co. Ltd..

Appendix A. Supplementary data

Supplementary data to this article can be found online at https://doi.org/10.1016/j.net.2022.11.003.

APPENDIX A. Decay heat of assemblies from Ringhals-2 and Ringhals-3

Table A1
Decay heat calculation with STREAM energy release models.

Reactor name	ID (wt.%^{235}U)	Burnup (GWd/MTU)	Cooling time (days)	Measured decay heat and uncertainty		Calculated decay heat from STREAM with different energy release model		
				Measured (W)	2σ (W)	CONSTK[a] (W)	OTFKCQ[b] (W)	OTFKVQ[c] (W)
Ringhals-2 (15 × 15 assembly)	C01 (3.1)	36.7	8468	415.8	11.65	417.9	421.6	422.5
	C12 (3.1)	36.4	8403	410.3	11.57	412.9	416.5	417.4
	C20 (3.1)	35.7	6950	415.8	11.65	**429.6**[d]	**433.6**[d]	**434.5**[d]
	C42 (3.1)	35.6	5803	442.3	12.04	440.6	444.8	445.8
	D27 (3.3)	39.7	7673	456.1	12.24	448.4	452.3	453.3
	D38 (3.3)	39.4	8005	442.3	12.04	439.5	443.3	444.3
	E38 (3.2)	34.0	7999	376.3	11.07	369.7	373.0	373.8
	E40 (3.2)	34.3	8075	381.3	11.14	373.6	376.9	377.7
	F14 (3.2)	34.0	7726	381.8	11.15	378.4	381.8	382.5
	F21 (3.2)	36.3	7376	420.9	11.12	413.4	417.1	418.0
	F25 (3.2)	35.4	7729	396.7	11.37	396.5	400.0	400.9
	F32 (3.2)	51.0	5860	692.0	15.73	691.9	697.7	699.6
	G11 (3.2)	35.5	6990	416.4	11.66	408.5	412.2	413.1
	G23 (3.2)	35.6	6984	420.6	11.72	414.3	418.0	418.9
	I09 (3.2)	40.2	5849	507.9	13.01	510.2	514.7	515.9
	I20 (3.2)	34.3	6588	403.5	11.47	396.0	399.5	400.4
	I24 (3.2)	34.3	6601	410.1	11.56	**397.0**[d]	400.6	401.4
	I25 (3.2)	36.9	6198	445.8	12.09	445.2	449.2	450.1
Ringhals-3 (17 × 17 assembly)	0C9 (3.1)	38.4	6551	491.2	12.76	500.4	**504.3**[d]	**505.7**[d]
	0E2 (3.1)	41.6	5823	587.9	14.19	582.6	587.2	588.9
	0E6 (3.1)	36.0	5829	487.8	12.71	484.0	487.9	489.2
	1C2 (3.1)	33.3	6559	417.7	11.68	416.9	420.5	421.5
	1C5 (3.1)	38.5	6593	499.2	12.88	500.0	503.8	505.2
	1E5 (3.1)	34.6	5818	468.8	12.43	464.9	468.7	469.9
	2A5 (2.1)	20.1	7297	233.8	8.96	235.2	237.1	237.6
	2C2 (3.1)	36.6	6550	466.5	12.40	466.1	470.0	471.3
	3C1 (3.1)	36.6	6545	470.2	12.45	466.2	470.1	471.4
	3C5 (3.1)	38.4	6543	501.4	12.91	499.5	503.3	504.7
	3C9 (3.1)	36.6	6552	468.4	12.43	465.8	469.7	471.0
	4C4 (3.1)	33.3	6572	422.0	11.74	416.9	420.5	421.6
	4C7 (3.1)	38.4	6549	498.7	12.87	499.3	503.1	504.5

Table A1 (*continued*)

Reactor name	ID (wt.%^{235}U)	Burnup (GWd/MTU)	Cooling time (days)	Measured decay heat and uncertainty		Calculated decay heat from STREAM with different energy release model		
				Measured (W)	2σ (W)	CONSTK[a] (W)	OTFKCQ[b] (W)	OTFKVQ[c] (W)
	5A3_1 (2.1)	19.7	6972	237.7	9.02	233.5	235.4	235.9
	5A3_2 (2.1)	19.7	6975	236.7	9.00	233.5	235.4	235.9
	5A3_3 (2.1)	19.7	6977	243.4	9.10	233.5	235.4	235.9
	5A3_4 (2.1)	19.7	7291	230.9	8.92	**230.1**[d]	232.0	232.4
	5A3_5 (2.1)	19.7	7304	230.3	8.91	229.9	231.8	232.3

[a] CONSTK mode in STREAM, fixed Kappa values.
[b] On-the-fly energy release model with constant q_c (OTFKCQ).
[c] On-the-fly energy release model with explicit neutron-photon heating (OTFKVQ).
[d] Calculated result outside the range of measurement uncertainty.

REFERENCES

[1] J. Sterbentz, Q-Value (MeV/fission) Determination for the Advanced Test Reactor, Idaho National Laboratory (INL), 2013. No. INL/EXT-13-29256.
[2] D.P. Griesheimer, S.J. Douglass, M.H. Stedry, Self-consistent energy normalization for quasistatic reactor calculations, Journal of Nuclear Engineering 2 (2) (2021) 215–224.
[3] L. Ghasabyan, K. Mikityuk, J. Krepel, S. Pelloni, Use of SERPENT Monte-Carlo code for development of 3D full-core models of Gen-IV fast spectrum reactors and preparation of safety parameters/cross-section data for transient analysis with FAST code system, in: Proceedings of the International Conference on Fast Reactors and Related Fuel Cycles: Safe Technologies and Sustainable Scenarios (FR13), 2013. Paris, March.
[4] K.S. Kim, K.T. Clarno, Y. Liu, et al., Neutron Capture Energies for Flux Normalization and Approximate Model for Gamma-Smeared Power, Oak Ridge National Lab (ORNL), 2018. No. ORNL/SPR-2017/471.
[5] J. Rhodes, K. Smith, Z. Xu, CASMO-5 energy release per fission model, in: Proceedings of PHYSOR2008, 2008. Switzerland. September 14-19.
[6] J. Rhodes, K. Smith, D. Lee, CASMO-5 development and applications, in: Proceedings of the PHYSOR-2006 Conference, ANS Topical Meeting on Reactor Physics, Canada, Vancouver, BC, 2006.
[7] M.B. Chadwick, M. Herman, P. Obložinský, et al., ENDF/B-VII. 1 nuclear data for science and technology: cross sections, covariances, fission product yields and decay data, Nucl. Data Sheets 112 (12) (2011) 2887–2996.
[8] S. Choi, D. Lee, Three-dimensional method of characteristics/diamond-difference transport analysis method in STREAM for whole-core neutron transport calculation, Comput. Phys. Commun. 260 (2021), 107332.
[9] S. Choi, W. Kim, J. Choe, et al., Development of high-fidelity neutron transport code STREAM, Comput. Phys. Commun. 264 (2021), 107915.
[10] J. Leppänen, T. Kaltiaisenaho, V. Valtavirta, M. Metsälä, Development of a coupled neutron/photon transport mode in the serpent 2 Monte Carlo code, in: International Conference on Mathematics and Computational Methods Applied to Nuclear Science and Engineering, M&C, Jeju, Korea, 2017. April 16-20.
[11] C. Liegeard, A. Calloo, G. Marleau, E. Girardi, Impact of photon transport on power distribution, in: Proceedings of the International Conference on Mathematics and Computational Methods Applied to Nuclear Science and Engineering, M&C 2017, Jeju, Korea, 2017. April 16-20.
[12] AREVA NP INC, The ARCADIA® reactor analysis system for PWRs methodology description and benchmarking results, Tech. rep (2010) 10–11. Areva NP Inc, March.
[13] Y. Liu, R. Salko, K.S. Kim, et al., Improved MPACT energy deposition and explicit heat generation coupling with CTF, Ann. Nucl. Energy 152 (2021), 107999.
[14] B.A. Lindley, J.G. Hosking, P.J. Smith, et al., Current status of the reactor physics code WIMS and recent developments, Ann. Nucl. Energy 102 (2017) 148–157.
[15] S. Jae, N. Choi, H.G. Joo, Implementation and verification of explicit treatment of neutron/photon heating in nTRACER, in: Proceedings of ICAPP 2020, Abu Dhabi, UAE, 2020. March 15-19.
[16] R. Tuominen, V. Valtavirta, J. Leppänen, New energy deposition treatment in the Serpent 2 Monte Carlo transport code, Ann. Nucl. Energy 129 (2019) 224–232.
[17] OpenMC Theory and Methodology https://docs.openmc.org/en/stable/methods/index.html.
[18] T. Goorley, M. James, T. Booth, et al., Initial MCNP6 release overview, Nucl. Tech. 180 (3) (2012) 298–315.
[19] D.H. Lee, J.S. Kim, S.K. Lim, H.J. Shim, McCARD gamma transport analysis for RFNC photon spectrum benchmark, in: Transactions of the Korean Nuclear Society Autumn Meeting, 2018. Yeosu, Korea, October 25-26.
[20] M. Lemaire, H. Lee, P. Zhang, D. Lee, Interpretation of two SINBAD photon-leakage benchmarks with nuclear library ENDF/B-VIII. 0 and Monte Carlo code MCS, Nucl. Eng. Technol. 52 (7) (2020) 1355–1366.
[21] F.B. Brown, R.D. Mosteller, W.R. Martin, Monte Carlo-Advances and Challenges, Los Alamos National Lab (LANL), Los Alamos, NM (United States), 2008. LA-UR-08-05891.
[22] N.N.T. Mai, K. Kim, M. Lemaire, et al., Analysis of several VERA benchmark problems with the photon transport capability of STREAM, Nucl. Eng. Technol. 54 (7) (2022) 2670–2689.
[23] A.T. Godfrey, VERA Core Physics Benchmark Progression Problem Specifications, CASL Technical Report: CASL-U-2012-0131-004, 2014.
[24] B. Ebiwonjumi, S. Choi, M. Lemaire, D. Lee, H.C. Shin, Validation of lattice physics code STREAM for predicting pressurized water reactor spent nuclear fuel isotopic inventory, Ann. Nucl. Energy 120 (2018) 431–449.
[25] B. Ebiwonjumi, S. Choi, M. Lemaire, et al., Verification and validation of radiation source term capabilities in STREAM, Ann. Nucl. Energy 124 (2019) 80–87.
[26] NuScale Plant Design Overview, U.S. Nuclear Regulatory Commission, 2012. NP-ER-0000-1198.
[27] S.K. Lee, et al., Nuclear Design Report for Yonggwang Unit 3, Cycle 1, Korea Atomic Energy Research Institute (KAERI), 1995. September.
[28] R. Sher, C. Beck, Fission-energy Release for 16 Fissioning Nuclides. Final Report (No. EPRI-NP-1771). Stanford Univ., Dept. of Mechanical Engineering, CA (USA), 1981.
[29] A. Trkov, D.A. Brown, ENDF-6 Formats Manual: Data Formats and Procedures for the Evaluated Nuclear Data Files (No. BNL-203218-2018-INRE), Brookhaven National Lab.(BNL), Upton, NY (United States), 2018.
[30] K. Kim, M. Lemaire, N.N.T. Mai, et al., Generation of a multigroup gamma production and photon transport library for STREAM, in: Transactions of the Korean Nuclear Society Virtual Spring Meeting, 2020. July 09-10.
[31] A.C. Kahler III, R. Macfarlane, NJOY2016, Los Alamos National Lab (LANL), 2016, Los Alamos, NM (United States), No. NJOY, NJOY16; 005075MLTPL00.
[32] H. Lee, W. Kim, P. Zhang, M. Lemaire, et al., Mcs - a Monte Carlo particle transport code for large-scale power reactor analysis, Ann. Nucl. Energy 139 (2020), 107276.
[33] X. Wang, Y. Liu, W. Martin, et al., Energy deposition analysis for VERA progression problems by MCNP, in: Proceedings of PHYSOR 2018, Cancun, Mexico, 2018.
[34] D.A. Brown, M.B. Chadwick, R. Capote, et al., ENDF/B-VIII. 0: the 8th major release of the nuclear reaction data library with CIELO-project cross sections, new standards and thermal scattering data, Nucl. Data Sheets 148 (2018) 1–142.
[35] S. Choi, C. Lee, D. Lee, Resonance treatment using pin-based pointwise energy slowing-down method, J. Comput. Phys. 330 (2017) 134–155.
[36] S. Kinast, D. Tomatis, Energy deposition in coolant of PWR under normal operation and accident conditions, Nucl. Eng. Des. 384 (2021), 111479.
[37] D. Lee, J. Rhodes, K. Smith, Quadratic depletion method for gadolinium isotopes in CASMO-5, Nucl. Sci. Eng. 174 (1) (2013) 79–86.
[38] J. Jang, B. Ebiwonjumi, W. Kim, et al., Validation of spent nuclear fuel decay heat calculation by a two-step method, Nucl. Eng. Technol. 53 (1) (2021) 44–60.
[39] Swedish Nuclear Fuel and Waste Management Company. Measurements of Decay Heat in Spent Nuclear Fuel at the Swedish Central Interim Storage Facility, Clab. ISSN 1402-3091. SKB Rapport R-05-62.
[40] I.C. Gauld, G. Ilas, B.D. Murphy, C.F. Weber, Validation of SCALE 5 Decay Heat Predictions for LWR Spent Nuclear Fuel. Nuclear Regulatory Commission report (ORNL/TM-2006/13).